

Production of intense radioactive beams at ISAC using low-energy protons

M. Trinczek, S. Lapi, B. Guo, F. Ames, K.R. Buckley, J.M. D'Auria, K. Jayamanna, W.P. Liu, C. Ruiz, and T.J. Ruth

Abstract: A proof-of-principle approach for the production of intense ($\sim 10^8/s$) radioactive ion beams, which differs from the standard ISOL (Isotope Separation On-Line) technique, has been demonstrated successfully using ^{11}C at the TRIUMF laboratory. This approach uses 13 MeV protons produced by a medical cyclotron and should be useful for a range of radioisotopes of interest to the nuclear astrophysics research programme.

PACS No.: 29.25.Rm

Résumé : Nous démontrons une preuve de faisabilité d'une méthode de production d'intenses faisceaux ($\sim 10^8/s$) d'ions radioactifs, différente de la technique standard ISOL (séparation isotopique en ligne) en générant un faisceau de ^{11}C au laboratoire TRIUMF. Cette approche utilise les protons de 13 MeV produits par un cyclotron médical et devrait être utile pour un domaine de radioisotopes intéressant les chercheurs en astrophysique nucléaire.

[Traduit par la Rédaction]

1. Introduction

Radioactive heavy-ion beams are now used in a variety of laboratories around the world for a broad spectrum of studies in the fields of fundamental symmetries, nuclear astrophysics, condensed-matter physics, nuclear structure, and other related fields. The same radioisotopes are also of importance to nuclear medicine. The TRIUMF ISAC (Isotope Separation and ACcelerator) facility in Vancouver, Canada has proven to be a world leader in these fields, producing intense beams of select isotopes of interest [1, 2].

There are two main approaches used at major laboratories today to produce radioactive beams, namely, the ISOL (Isotope Separation On-Line) technique and the In-Flight Fragmentation technique. The former involves the interaction of some projectile (e.g., proton, neutron, heavy ion) onto a thick target; operation of the target at high temperatures ($\sim 1500\text{ }^\circ\text{C}$) leads to diffusion of reaction products

Received 1 November 2005. Accepted 16 April 2006. Published on the NRC Research Press Web site at <http://cjp.nrc.ca/> on 2 August 2006.

M. Trinczek,¹ F. Ames, K.R. Buckley, K. Jayamanna, C. Ruiz,² and T.J. Ruth. TRIUMF, Vancouver, BC V6T 2A3, Canada.

S. Lapi and J.M. D'Auria. Simon Fraser University, Burnaby, BC V5A 1S6, Canada.

B. Guo and W.P. Liu. China Institute of Atomic Energy, Beijing 102413, China.

¹Corresponding author (e-mail: trin@triumf.ca).

²Also at: Simon Fraser University, Burnaby, BC V5A 1S6, Canada.

Table 1. Calculated production rates in a thick target using 50 μA of 13 MeV protons for some desired species.

Isotope	Half-life	Target material	Production reaction	Rate of production (s^{-1})	Desired intensity at experiment (s^{-1})
^{11}C	20.39 min	$\text{N}_2(\text{g})$	$^{14}\text{N}(\text{p},\alpha)^{11}\text{C}$	2.4×10^{11a}	$10^7 - 10^9$
^{14}O	70.606 s	$\text{N}_2(\text{g})$	$^{14}\text{N}(\text{p},\text{n})^{14}\text{O}$	2×10^{10b}	$10^5 - 10^6$
^{15}O	122.24 s	$^{15}\text{N}_2(\text{g})$	$^{15}\text{N}(\text{p},\text{n})^{15}\text{O}$	2.1×10^{11a}	$10^8 - 10^{11}$
^{13}N	9.965 min	$\text{O}_2(\text{g})$	$^{16}\text{O}(\text{p},\alpha)^{13}\text{N}$	4.8×10^{10a}	$10^8 - 10^9$
^{17}F	64.46 s	$\text{Ne}(\text{g})$	$^{20}\text{Ne}(\text{p},\alpha)^{17}\text{F}$	1.5×10^{8c}	$10^8 - 10^9$

^aFrom IAEA at http://www-nds.iaea.org/medical/positron_emitters.html.

^bRef. 6.

^cFrom W. Gruhle and B. Kober. Nucl. Phys. A, **286**, 523 (1977).

into an ion source. The correct choice of product element, target material matrix, and ion source leads to an ion beam of a particular element, with the isotope selected by an on-line magnetic analyzer. The extracted radioactive ion beam can then be electrostatically accelerated to the desired energy. The latter production technique generally involves the fragmentation of a very energetic (>100 MeV/u) heavy-ion beam and the use of appropriate electromagnetic devices to select the isotope of interest. These two approaches produce beams with complementary characteristics and are used in different types of experimental programmes.

The ISAC radioactive beams facility uses the ISOL approach and has been successful producing intense beams of certain exotic isotopes such as $^{8,9,11}\text{Li}$, ^{21}Na , and ^{74}Rb . However, it has proven difficult to produce certain isotopes of importance to the experimental nuclear astrophysics programme such as ^{11}C , ^{13}N , ^{14}O , and ^{15}O in sufficient required intensities, i.e., of the order of 10^8 /s or greater.

Recently, a new approach was developed at the Lawrence Berkeley National Laboratory in which two (^{11}C , ^{14}O) of these isotopes of interest have been produced in reasonable intensities as accelerated radioactive beams using low-energy protons as the production system [3, 4]. This approach is an extension of methods used for many years for the production of similar radioisotopes for usage in nuclear medicine applications such as PET (Positron Emission Tomography) [5].

It was decided to pursue a similar approach at the TRIUMF ISAC facility and the results of these proof-of-principle studies are described herein. It should be mentioned that a successful approach would allow radioactive beams to be produced without using the TRIUMF 500 MeV main cyclotron and could lead to two different methods of producing radioactive beams at ISAC. These two beams could, in turn, be used simultaneously for different experimental applications, increasing the amount of available beam time.

An important aspect of this approach is that it can be used to produce beams of isotopes that are of value to the scientific programme and which can be made in high intensities with low-energy protons. A list of some beams needed for approved experiments at TRIUMF with proposed methods and calculated rates of production from reported cross sections are presented in Table 1. The majority of the experiments are scattering and nucleon-transfer types of studies.

2. Experimental design

This approach involves the irradiation of a gaseous target of appropriate composition using low-energy (~ 13 MeV) protons, fast chemical and (or) physical separation of the product of interest, transfer of the gaseous product to either the inlet of the on-line ISAC ion source or to the inlet of OLIS (Off-Line Ion Source) [7], ionization, and then subsequent acceleration to the experimental apparatus as shown in Fig. 1.

Fig. 1. Schematic of the proposed production process.

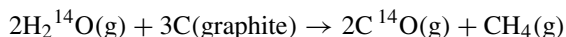
The overall experiment was divided into three phases. The first phase was to investigate the overall efficiency of the production, the chemical and (or) physical separation and the transfer of the desired radioisotope. The second phase was needed to understand how best to inject the gaseous species produced in phase one into the ion source. The third phase combined the previous results to extract an actual radioactive ion beam from this alternative approach.

3. Experimental procedures and results

3.1. Phase 1: ^{14}O production and transfer

The first phase involved a study to demonstrate and measure the overall efficiency of the first steps of this process, namely, the production, the chemical separation, and the transfer. This study was performed using the radioisotope, ^{14}O ($t_{1/2} = 70.606$ s), and full details of it are available in the thesis work of Lapi [6].

The ^{14}O was made using the $^{14}\text{N}(p,n)^{14}\text{O}$ reaction with protons having energies in the range of 13 MeV. The target chamber contained 5% $\text{H}_2(\text{g})$ in natural $\text{N}_2(\text{g})$ at a pressure of 2.1 MPa. The product of these irradiations was $\text{H}_2^{14}\text{O}(\text{g})$, which was transferred from the target area to a nearby fume hood for on-line processing. Flowing the target gas with the $\text{H}_2^{14}\text{O}(\text{g})$ through activated charcoal at high temperature (1100 °C) converts the ^{14}O to $\text{CO}(\text{g})$



The H_2^{14}O was converted to C^{14}O as it was expected that this molecule would provide higher overall efficiencies for the transfer and the subsequent ionization.

After the oven, the gas was passed over a soda-lime trap to remove unconverted $\text{H}_2^{14}\text{O}(\text{g})$ and then through a molecular sieve at liquid-nitrogen temperatures to retain the $\text{C}^{14}\text{O}(\text{g})$ while allowing the bulk $\text{N}_2(\text{g})$ and $\text{H}_2(\text{g})$ target gas to pass. The efficiency of this step is ~92%.

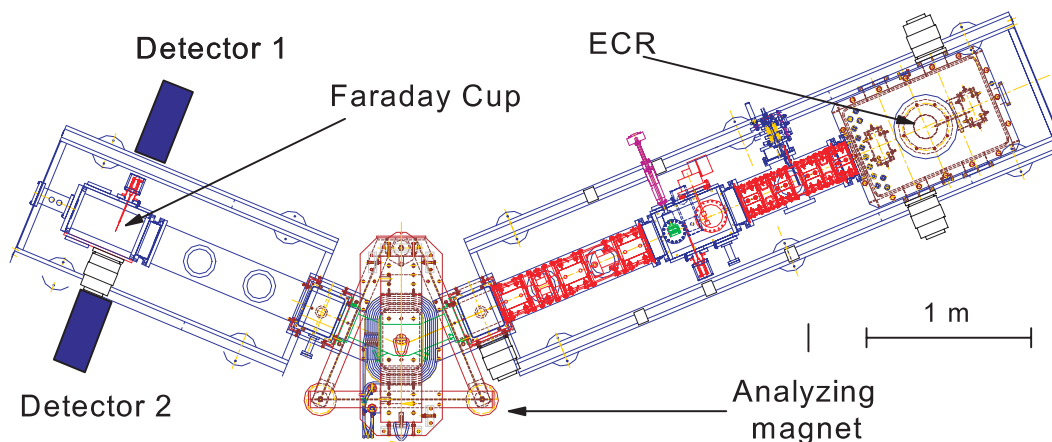
The next step is the transfer to the ion source. Studies performed exhibit an overall efficiency (for all steps) of about 2% if the length of the transfer line (1/4 in. inner diameter (1 in. = 2.54 cm)) is 200 m (the expected length between the production and ionization sites). It should be noted that a higher efficiency (7%) was measured if $\text{H}_2\text{O}(\text{g})$ was transferred directly without chemical manipulation. The ^{14}O radioactivity was detected using its characteristic 2313 keV gamma ray.

Based upon this, the total rate that could be introduced into the ion source is $\sim 4 \times 10^8$ ^{14}O /s. Coupled with the expected efficiency (up to 10%) of OLIS and of the ISAC accelerator (~33%), the resultant beam flux available for experimental purposes is estimated to be $\sim 1.3 \times 10^7$ ^{14}O /s.

3.2. Phase 2: ^{13}C stable beam at the ISAC Test Stand

A second phase was mounted to understand how to integrate the gaseous species into the ISAC ECR (Electron Cyclotron Resonance) ion source [8]. The ECR was a new design that had not been tested with a wide variety of different species; consequently, it was decided to use the off-line ECR ion source of equivalent design located at the ISAC Test Stand [9] where more time was available for development. A plan view of the ISAC Test Stand is displayed in Fig. 2. Carbon was chosen as the first species to be ionized and accelerated since it had an isotope of interest with a reasonable half-life (^{11}C , see Table 1) as well as its stable ^{13}C isotope, which could be easily used at the Test Stand.

Fig. 2. Plan view of the ISAC Test Stand at TRIUMF showing the layout of the ECR, extraction and steering optics, analyzing magnet, Faraday cup, and detectors employed in the study.



Three different experiments using the ISAC Test Stand were performed. The purpose of the first experiment was to assess whether this ECR could produce a measurable beam of carbon as $^{13}\text{C}^+$, $^{13}\text{CO}^+$, $^{13}\text{CO}^{2+}$, . . . , from a ^{13}C -enriched sample of CO_2 (^{13}C , 99%-enriched in carbon dioxide form, Cambridge Isotope Laboratories, Inc.).

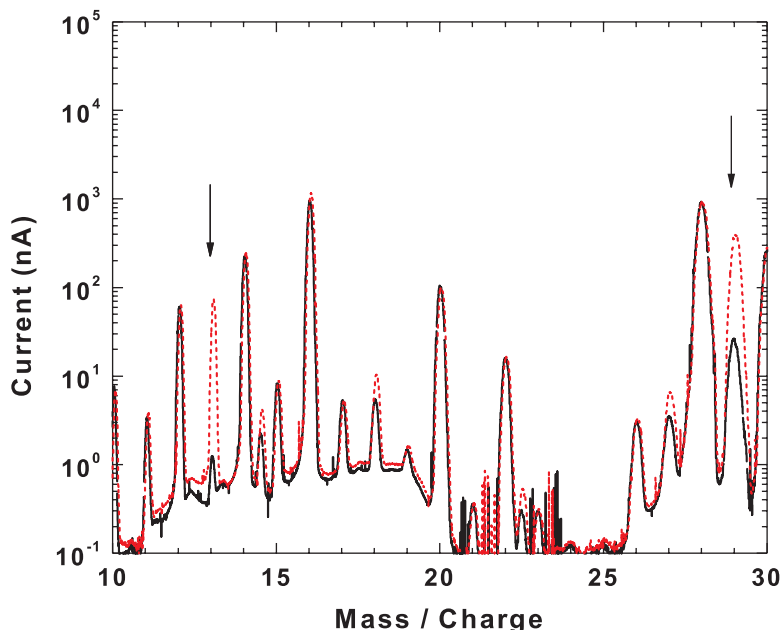
Here, the off-line ECR was started with He and allowed to stabilize; He is used as a support gas in the ECR operation. Its performance was checked with a standard calibrated leak of Ne; ^{22}Ne is typically used to gauge the operation of the source and has an efficiency of $\sim 2.5\%$. (All efficiencies are calculated with respect to the amount of a species admitted into the ion source to the extracted ion beam current measured at the Faraday cup, located after the analyzing magnet, as shown in Fig. 2.) Then, increasing amounts of $^{13}\text{CO}_2$ were admitted into the system and extracted ion beam currents were measured at the Faraday Cup. This was done at different mass positions and it was evident that by adjusting the relative amount of $^{13}\text{CO}_2$ admitted into the system, the currents would change.

The $^{13}\text{CO}_2$ was then removed from the system and a mass scan of the background gas in the ECR, running only on He, was recorded (some residual Ne would be in the system). The $^{13}\text{CO}_2$ was then put back into the system and a second mass scan was taken. These two mass scans are shown in Fig. 3 and it is clear that the peaks at Mass/Charge position 13 ($^{13}\text{C}^+$) and 29 ($^{13}\text{CO}^+$) correspond to the admitted $^{13}\text{CO}_2$. There is also a small increase at the Mass/Charge position of 14.5 ($^{13}\text{CO}^{2+}$) and a small peak was observed at a Mass/Charge position of 45 ($^{13}\text{CO}_2^+$, not shown).

The second experiment measured the ionization efficiency of the ECR system for carbon. Ideally, a known calibrated leak of ^{13}C as either $^{13}\text{CO}_2$ or ^{13}CO should be used, but one was not available; as such, this measurement was performed indirectly, relating to a calibrated bottle using the well-understood efficiency of ^{22}Ne in the system. Based on repeatable measurements over several days, the efficiency for $^{13}\text{C}^+$ was estimated to be $\sim 10\%$ and for $^{13}\text{CO}^+$ it was estimated to be $\sim 30\%$ for the stable isotope on the Test Stand.

The third experiment performed at the Test Stand tested the apparatus necessary for the future ^{11}C measurements. In particular, it was desirable to know how long the sample of approximately 10 mL volume would last and if the residual sample gas would overwhelm the ECR plasma. A radioactive sample of $^{11}\text{CO}_2$ (as detailed in Sect. 3.3) was prepared and allowed to decay away completely. It was then installed on the Test Stand ECR system, connected to a mass-flow controller. The ECR was started with He, allowed to stabilize and its performance checked with Ne. A small amount of the sample was admitted at a relatively low flow rate and did not extinguish the ECR.

Fig. 3. Mass scan illustrating the injection of $^{13}\text{CO}_2$ into the Test Stand ECR. The continuous line represents the mass peaks from the residual gas in the ECR system. The dotted line represents the mass peaks when $^{13}\text{CO}_2$ is added; the peaks at Mass/Charge positions of 13 ($^{13}\text{C}^+$) and 29 ($^{13}\text{CO}^+$), highlighted by the arrows, correspond to the admitted $^{13}\text{CO}_2$.



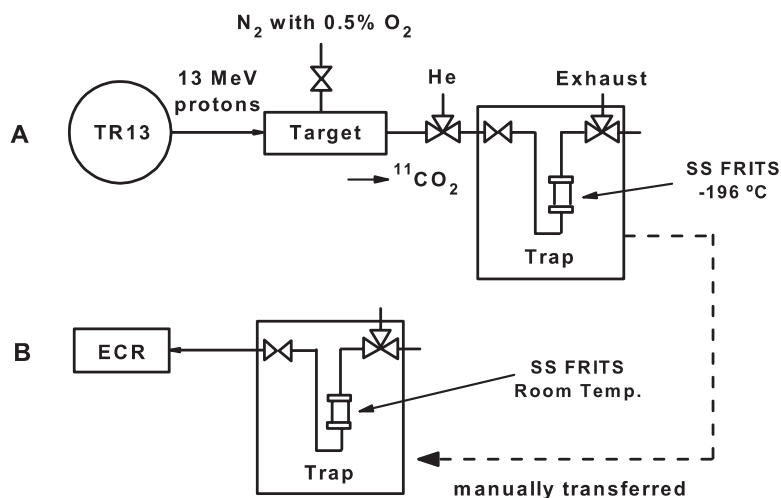
A few quick mass scans were taken of the sample and of the background to note the difference of the sample being open or closed. Residual amounts of gas such as nitrogen and oxygen (from the preparation of the sample) were observed. Then the ECR plasma was allowed to run with this small flow of sample gas into the system and the readback of the mass-flow controller monitored. The readback signal stayed constant as long as there was sufficient gas in the sample, then it decreased. In total, this took just more than 1 h, which was deemed a satisfactory length of time to admit the complete sample volume. Given its half-life, it would be better to admit the radioactive ^{11}C ($t_{1/2} = 20.39$ min) sample more quickly in the future experiments to produce as intense a beam as possible, so the flow rate was adjusted accordingly for the radioactive samples.

3.3. Phase 3: ^{11}C at the ISAC Test Stand

The final phase of the development involved the actual production of an ion beam of ^{11}C . Two experiments were performed in a similar fashion, to ensure the repeatability of the method, though under different operating conditions. The base pressure of the ECR chamber was different by an order of magnitude, leading to different performance. The ^{11}C was produced through the $^{14}\text{N}(p,\alpha)^{11}\text{C}$ reaction, in the form of $^{11}\text{CO}_2$ that was generated using a 13 MeV proton beam from the TR13 medical cyclotron to irradiate a gaseous target of 0.5% O_2 in natural N_2 . The $^{11}\text{CO}_2$ was then trapped on a stainless steel frit at the temperature of -196 °C and the frit was purged with He to remove the target gas. The sample was then isolated and allowed to warm to room temperature. A schematic diagram of the production system is shown in Fig. 4.

The frit assembly containing the $^{11}\text{CO}_2$ sample was transferred manually to the Test Stand ECR source and connected to a mass-flow controller inlet. The ECR source was started with the He support gas and allowed to stabilize; its performance was checked with a standard calibrated leak of Ne. The $^{11}\text{CO}_2$ was then injected into the ECR source through the mass-flow controller at a flow rate anticipated

Fig. 4. Schematic diagram of the $^{11}\text{CO}_2$ production system used to make a beam of ^{11}C at TRIUMF. Configuration A shows the sample trap hooked up to the production target for loading. Once loaded and purged with He, the sample trap is manually transferred to the ECR system and connected to an inlet via a mass-flow controller, as shown in configuration B.



to consume the sample in 20–30 min. The ion beam was extracted with a 30 kV bias on the ECR system and $^{11}\text{CO}^+$ was separated with the mass analyzer at a Mass/Charge position of 27 as this represented the highest of the ^{11}C -labeled species from the ion source. The measurement focused on the overall ECR efficiency and the observed beam intensity.

The radioactivity implanted on the Faraday cup was measured by two detectors. A NaI(Tl) detector (Harshaw integral line Type 12S12, 3 in. \times 3 in.) was placed at a right angle near (~ 7.5 in.) the Faraday cup (refer to Fig. 2) and a second detector (BICRON Model 2M2, 2 in. \times 2 in.) was employed at 180° in summed singles mode. The second detector was also run in coincidence only to verify that the measured radioactivity was indeed 511 keV annihilation gamma rays from the positron decay of ^{11}C , but these data were not used for analysis.

To determine the beam intensity $I(t)$, let N_i be the number of undecayed nuclei at the start of time bin i and $F = \{e^{-\Delta t/\tau}$ be the fraction of N_i that do not decay during the time bin i , let $P_i = I_i \Delta t$ be the number of nuclei admitted during the i th time bin (of length Δt) and F' be the fraction of P_i that do not decay during the i th time bin, and let D_i be the number of decays during the i th time bin. Then

$$N_{i+1} = FN_i + F'P_i \quad (1)$$

and

$$D_i = (1 - F)N_i + (1 - F')P_i \quad (2)$$

$$D_{i+1} = (1 - F)N_{i+1} + (1 - F')P_{i+1} \quad (3)$$

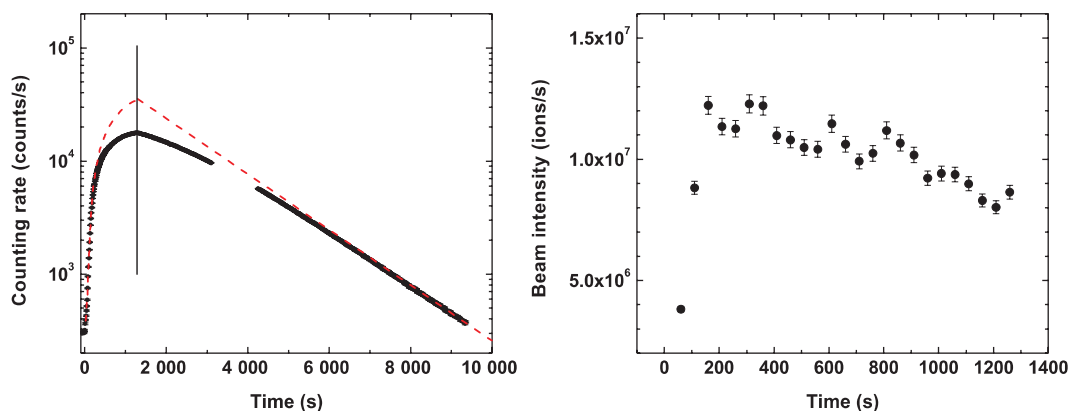
Substituting for N_i and using a bit of manipulation yields

$$D_{i+1} - FD_i = [(1 - F)F' - (1 - F')F]P_i + (1 - F')P_{i+1} \quad (4)$$

and assuming $P_i = P_{i+1}$ within the time bin Δt gives the beam intensity as

$$I(t) = \frac{D(t) - D(t - \Delta t)e^{-\Delta t/\tau}}{\Delta t(1 - e^{-\Delta t/\tau})} = R \frac{N_{\text{det}}(t) - N_{\text{det}}(t - \Delta t)e^{-\Delta t/\tau}}{\varepsilon_{\text{det}}Y\Delta t(1 - e^{-\Delta t/\tau})} \quad (5)$$

Fig. 5. Data and results from the first ^{11}C sample. The left panel shows the measured summed singles spectrum with the solid points representing the counting rate observed in both detectors as a function of time. The broken line represents the true counting rate as determined from the data; see text for explanation. The right panel shows the beam intensity obtained from the first sample as a function of the collection time.



where $N_{\text{det}}(t)$ represents the detected counts within the time bin of t to $t + \Delta t$ with a total photopeak efficiency for detecting 511 keV gamma rays of ε_{det} , a gamma yield of $Y = 1.9952$, and R is the ratio of the true counting rate compared with the measured counting rate (explained below).

The left panel of Fig. 5 shows the measured summed singles spectrum for the first ^{11}C sample run. The solid points represent the counting rate observed in both detectors as a function of time; the break in the points was simply due to switching to a different acquisition file. At $t = 0$ s, the sample of $(5.55 \pm 0.56) \times 10^2$ MBq ^{11}C radioactivity was opened to the source and measured at the Faraday cup. The radioactivity at the cup was allowed to grow until $t = 1300$ s (vertical line on Fig. 5) where an up-stream valve was closed, preventing further ^{11}C from reaching the Faraday cup. For $t \geq 1300$ s, the collected radioactivity was observed as it decayed away.

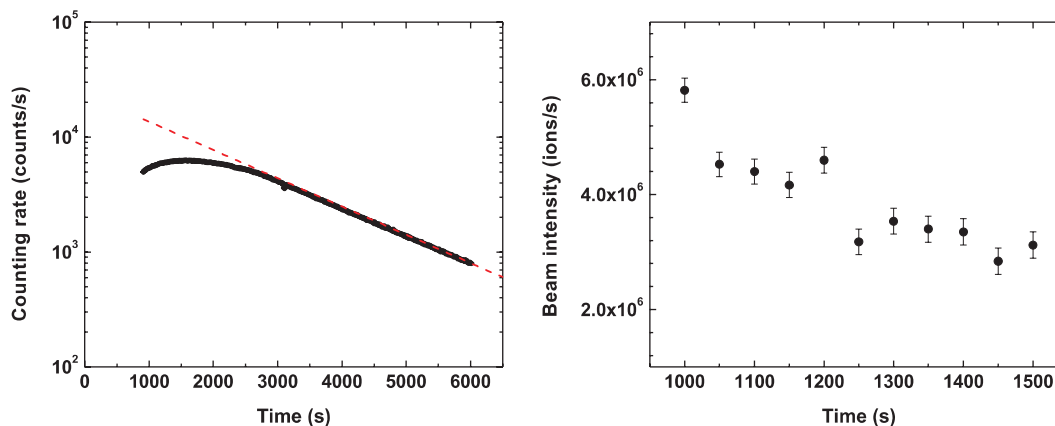
In this run, the instantaneous counting rate was too strong for the acquisition system; consequently, there is a deficit of observed counts, especially for higher counting rates. To remove this effect, R , the ratio of the true counting rate to the measured counting rate, was calculated from the data. At the end of the observation ($t \approx 9300$ s), the counting rate is relatively low, so this region was used to anchor an extrapolation back to $t = 1300$ s since it represents only the pure decay of any radioactivity that had been collected at the Faraday cup; illustrated by the broken line in Fig. 5. The ratio of this true counting rate compared with the measured counting rate was then calculated as a function of counting rate strength and applied to the data from $t = 0$ to $t = 1300$ s to generate the broken line in the growth portion of Fig. 5, which was used to determine the beam intensity.

With a ^{22}Na ($t_{1/2} = 2.6019$ years) source placed in the identical geometry as in the experiment, the combined detector gamma efficiency ε_{det} for the first run was found to be $(3.513 \pm 0.007) \times 10^{-3}$. With this detector efficiency and the data, (5) was used to determine the beam intensity during the collection time ($N_{\text{det}}(t)/\Delta t$ is the counting rate) and is shown in the right panel of Fig. 5. The average beam intensity for the first sample was determined to be $(9.9 \pm 0.4) \times 10^6$ ions/s.

The overall ECR source efficiency is calculated by comparing the amount of radioactivity detected at the Faraday cup, $A(t)_{\text{det}}$, to the amount of radioactivity presented to the source at $t = 0$ s ($A_0 = (5.55 \pm 0.56) \times 10^2$ MBq for the first run) with the equation

$$\varepsilon_{\text{source}} = \frac{A(t)_{\text{det}}}{\varepsilon_{\text{det}} Y A_0 e^{-t/\tau}} \quad (6)$$

Fig. 6. Data and results from the second ^{11}C sample. The left panel shows the measured summed singles spectrum with the solid points representing the counting rate observed in both detectors as a function of time. The broken line indicates the backwards extrapolation of the 20.39 min half-life of ^{11}C . The right panel shows the beam intensity obtained from the second sample as a function of the collection time.



In the case of the first run, an up-stream valve was closed (indicated in time by the vertical bar in the left panel of Fig. 5) preventing all of the presented ^{11}C radioactivity from reaching the Faraday cup. Thus, only a lower limit on the overall source efficiency for this sample run could be calculated; hence, $\varepsilon_{\text{source}} \geq (1.9 \pm 0.2)\%$.

A second run, under different ECR operating conditions was performed to check the repeatability of the production approach. Here, a sample of $(1.37 \pm 0.14) \times 10^3$ MBq was opened to the Test Stand ECR source and data recorded. To reduce the counting rate issues of the first run, 0.50 in. of Pb was placed in front of Detector 1 and 0.25 in. of Pb was placed in front of Detector 2. The new combined detector efficiency was determined to be $\varepsilon_{\text{det}} = (1.22 \pm 0.02) \times 10^{-3}$. Unlike the first run, this time the sample was allowed to fully deplete as the spectrum was recorded at the Faraday cup.

The left panel of Fig. 6 shows the measured summed singles spectrum for the second ^{11}C sample run. From (5), the beam intensity was extracted as a function of time and is shown in the right panel of Fig. 6. Since the reduced counting rate was not too strong for the acquisition system, the correction provided by R was not needed. The average beam intensity for the second sample was determined to be $(3.9 \pm 0.3) \times 10^6$ ions/s and the overall ECR source efficiency was calculated as $\varepsilon_{\text{source}} = (0.72 \pm 0.07)\%$ using (6). The results from the two runs differ due to the different ECR operating conditions.

Table 2 presents a summary of results from the two runs. Beams of ^{11}C were produced and monitored for tens of minutes. The difference between the measured ^{11}C and ^{13}C efficiencies are thought to be due to the very small amount of ^{11}C introduced to the ECR. Continuous injection of ^{11}C into the ECR by production of multiple ^{11}C batch samples may improve the efficiency. Based on these results, conservative estimates would lead to beam intensities $\sim 4 \times 10^8$ ions/s for ^{11}C radioactivity amounts (~ 1 Ci or 37 GBq) easily produced by the TR13 medical cyclotron. Such intensities, when delivered to experiments, would allow studies such as radiative proton capture at the DRAGON recoil mass spectrometer facility to begin [10].

4. Conclusion

These successful results clearly display that this method can be used to produce a radioactive ion beam of ^{11}C and other radioisotopes without using the 500 MeV proton beam from the main TRIUMF cyclotron. Using low-energy protons from a medical cyclotron, it is feasible to produce beam intensities

Table 2. Summary of results for the ^{11}C tests.

Run	Beam intensity	Source efficiency
1	$(9.9 \pm 0.4) \times 10^6$ ions/s	$\geq (1.9 \pm 0.2)\%$
2	$(3.9 \pm 0.3) \times 10^6$ ions/s	$(0.72 \pm 0.07)\%$

that would be useful to the research programme at the ISAC facility. The limitation on intensity at this point appears to be the efficiency of the currently available ion source.

Independent of the work reported here, TRIUMF plans to commission a new ECR ion source on OLIS and a newly designed FEBIAD (Forced Electron Beam Ion Arc Discharge) ion source for on-line experiments at the ISAC facility. It is intended to continue the studies on these ion sources when they become available, as higher ionization efficiencies are expected for the elements of interest. This will allow the development of a transfer line from the production cyclotron to the ion source and enable the continuous batch mode necessary for experiments.

Acknowledgments

The authors would like to thank the excellent TRIUMF research and technical staff for their support. In particular, we acknowledge the contributions of P.G. Bricault, D.A. Hutcheon, P. Machule, M. McDonald, D. Yuan, and A. Zyuzin. This work was supported in part by TRIUMF and the Natural Sciences and Engineering Research Council. B.G. acknowledges financial aid from the Major State Basic Research Development Program of China under Grant No. 2003CB716704 and the National Natural Science Foundation of China under Grant No. 10575137.

References

1. R.E. Laxdal. Nucl. Instrum. Methods B, **204**, 400 (2003).
2. M. Dombisky, P. Bricault, P. Schmor, and M. Lane. Nucl. Instrum. Methods B, **204**, 191 (2003).
3. J. Powell, R. Joosten, C.A. Donahue, R.F. Fairchild, J. Fujisawa, F.Q. Guo, P.E. Haustein, R.-M. Larimer, C.M. Lyneis, M.A. McMahan, D.M. Moltz, E.B. Norman, J.P. O'Neil, M.A. Ostas, M.W. Rowe, H.F. VanBrocklin, D. Wutte, Z.Q. Xie, X.J. Xu, and J. Cerny. Nucl. Instrum. Methods A, **455**, 452 (2000).
4. J. Powell, J.P. O'Neil, and J. Cerny. Nucl. Instrum. Methods B, **204**, 440 (2003).
5. K.R. Buckley, S. Jivan, and T.J. Ruth. Nucl. Med. Bio. **31**, 825 (2004).
6. S. Lapi. M.Sc. thesis, Simon Fraser University, Burnaby, BC. 2003.
7. K. Jayamanna, D. Yuan, T. Kuo, M. McDonald, P.W. Schmor, and G. Dutto. Rev. Sci. Instrum. **67**, 1061 (1996).
8. K. Jayamanna, D. Yuan, D. Bishop, D. Dale, M. Dombisky, T. Kuo, S. Kadantsev, R. Kietel, D. Louie, M. McDonald, M. Olio, P. Schmor, and E. Stuber. Rev. Sci. Instrum. **71**, 946 (2000).
9. D. Yuan, T. Kuo, G. Cojocar, K. Jayamanna, M. McDonald, P. Schmor, and Y. Yin. Rev. Sci. Instrum. **69**, 1194 (1998).
10. S. Engel, D. Hutcheon, S. Bishop, L. Buchmann, J. Caggiano, M.L. Chatterjee, A.A. Chen, J. D'Auria, D. Gigliotti, U. Greife, D. Hunter, A. Hussein, C.C. Jewett, A.M. Laird, M. Lamey, W. Liu, A. Olin, D. Ottewell, J. Pearson, C. Ruiz, G. Ruprecht, M. Trinczek, C. Vockenhuber, and C. Wrede. Nucl. Instrum. Methods A, **553**, 491 (2005).